

Supplemental Materials.

Mice, diet and bone marrow transplantation

WT (C57BL/6J) and *Ldlr*^{-/-} (B6.129S7-Ldlrtm1Her) mice were purchased from Jackson Laboratory. Bone marrow from WT (C57BL/6J) and *Lnk*^{-/-} mice¹ were transplanted into irradiated 7-8 week old female WT (C57BL/6J) or *Ldlr*^{-/-} (B6.129S7-Ldlrtm1Her) mice. For atherosclerosis study, female *Ldlr*^{-/-} recipient mice were fed a western type diet (TD88137, Harlan Teklad) for the indicated period of time. *Lyn*^{kd/kd} mice were generously provided by Dr. Margaret L. Hibbs from Alfred Medical Research and Education Precinct at Monash University.

Histology analysis and immunofluorescent staining of atherosclerotic lesion

Tissues and ascending aorta were serially paraffin sectioned and section were stained with Hematoxylin and eosin (H&E staining) for morphometric lesion analysis as previously described. The aortic lesion size of each mouse was calculated as the mean of the lesion areas in five aortic sections. Identification of macrophages, neutrophils, lymphocytes in atherosclerotic lesions were performed using anti-mouse CD107b (Mac-3) (BD), anti-mouse Ly-6G (BioRad) and anti-mouse CD3 (BioRad) respectively. Primary antibodies were incubated with tissue sections at 4^oC overnight. After three times of washing with PBS, sections were incubated with Alexa-594 or Alexa-488 (Life Technologies) at room temperature for 30 minutes. Sections were counterstained with DAPI to identify nuclei before mounting. Images were taken using Nikon microscope and quantification of the images was performed using Image J.

Monocyte infiltration experiment

To track newly recruited monocytes in atherosclerotic lesions in studying the monocyte infiltration, the Ly-6C^{hi} subset of monocytes was labeled with fluorescent beads as described previously². Briefly, mice were injected intravenously with 250ul clodronate-containing liposome (<http://www.clodronateliposomes.com/clodronate-liposomes/clodronate-liposomes>) to deplete monocytes 96 hours before harvesting the heart. After 48 hours, mice were injected with Fluoresbrite Plain YG microspheres (polysciences, FITC channel) with a total volume 250ul (1:4 dilution in PBS). After another 48 hours, peripheral blood samples were collected and analyzed by FACS to quantify the efficiency of beads labeling of Ly-6C^{hi} monocyte. Mice were then euthanized and heart and aortic tissues were process as described previously. The newly recruited beads labeled monocytes in atherosclerotic lesions were visualized by fluorescence microscope and quantified using Image J.

Thrombosis assays: Mouse carotid artery FeCl₃-injury model and tail vein bleeding⁶

For FeCl₃-injury thrombosis assay, mice were anesthetized with isoflurane and the carotid artery was exposed. A filter paper soaked in 5% FeCl₃ was applied to the artery for 3 minutes and then blood flow was monitored with an ultrasound flow probe (Transonics). The time to total occlusion was defined as from the time point when FeCl₃ filter paper was applied to a complete occlusion of the artery with zero blood flow. Under the circumstance when there was no complete occlusion of the vessel or the vessel re-opened after a partial thrombi formation in the lumen, the whole procedure was stopped at 40 minutes and the occlusion time was recorded as 40 minute. After the procedure, all mice were etherized immediately³ⁱ. Tail bleeding assays were performed on *Ldlr*^{-/-} mice transplanted with either WT or *Lnk*^{-/-} bone marrow cells who were fed on western type diet for 10 weeks. Mice were anesthetized with isofluorane with a 5mm segment of the distal tip of the tail was cut off. Tail bleeding times were defined as the time required for the bleeding to stop.

Complete blood count

Complete blood counts were performed using whole blood collected from retro-orbital bleeding. 10% volume of acid-citrate-dextrose (ACD) was used as the anticoagulant and 25ul whole blood was analyzed using a FORCYTE Veterinary Hematology Analyzer (Oxford Science, Inc.) .

Flow cytometry of platelet-leukocyte aggregates

100ul of whole blood was collected using retro-orbital bleeding and anti-coagulated with 10% volume of ACD. Red blood cells (RBCs) were lysed briefly at 4^oC for less than 1 minute, and washed with staining buffer⁴. Cells were then stained with CD45-Pacific blue (eBioscience), CD115-APC (eBioscience), Gr-1-PerCP cy5.5 (Ly6-C/G; BD Biosciences), CD11b-PE Cy7 (eBioscience) and CD41-FITC (eBioscience) at 1:500 dilution for 30 min on ice. The cells were washed with staining buffer, resuspended in FACS buffer and run on an LSRII flow cytometer (BD Biosciences) to detect platelet Ly-6C^{hi} monocyte aggregates defined as CD45⁺Gr-1^{hi}CD115⁺CD41⁺, platelet Ly-6C^{lo} monocyte aggregates defined as CD45⁺Gr-1^{lo}CD115⁺CD41⁺ and platelet neutrophil aggregates defined as CD45⁺Gr-1⁺CD115⁻CD41⁺. Leukocyte activation was further analyzed as reflected by mean fluorescent intensity (MFI) of CD11b.

Flow cytometry of hematopoietic stem cell profile in mouse bone marrow and spleen, and human cord blood

Bone marrow and spleen cells were stained and analyzed as previously described⁵. Briefly, bone marrow cells from mouse femurs and tibias were stained with a cocktail of antibodies to lineage-committed cells (CD45R, CD19, CD11b, CD3e, TER-119, CD2, CD8, CD4 and Ly-6C/G, all FITC conjugated; Bioscience), Sca 1-Pacific blue and c-Kit-APC cy7 to identify LSK ($\text{Lin}^- \text{Sca1}^+ \text{c-Kit}^+$) cells and HPC ($\text{Lin}^- \text{Sca1}^- \text{c-Kit}^+$) cells. Further, another set of antibodies including a cocktail of antibodies to lineage-committed cells (same as mentioned above), Sca-1-FITC, CD16/CD32 (FcγRII/III)-Pacific blue, CD34-PerCP Cy5.5, CD71-PE and CD41-PE cy7 to identify progenitor cell populations including CMP ($\text{Lin}^- \text{Sca1}^- \text{c-Kit}^+ \text{CD34}^{\text{int}} \text{FcγRII/III}^{\text{int}}$), GMP ($\text{Lin}^- \text{Sca1}^- \text{c-Kit}^+ \text{CD34}^{\text{int}} \text{FcγRII/III}^{\text{hi}}$) and MEP ($\text{Lin}^- \text{Sca1}^- \text{c-Kit}^+ \text{CD34}^{\text{int}} \text{FcγRII/III}^{\text{low}}$) cell populations. In MEP population, ErP was defined as ($\text{Lin}^- \text{Sca1}^- \text{c-Kit}^+ \text{CD34}^{\text{int}} \text{FcγRII/III}^{\text{int}} \text{CD71}^+ \text{CD41}^-$) and MkP as ($\text{Lin}^- \text{Sca1}^- \text{c-Kit}^+ \text{CD34}^{\text{int}} \text{FcγRII/III}^{\text{int}} \text{CD71}^- \text{CD41}^+$)^{5,6}. In mouse spleen, similar staining and gating strategy were used in separating spleen LSK and HSPC. Spleen MkP was defined as ($\text{Lin}^- \text{Sca1}^- \text{c-Kit}^+ \text{CD41}^+$). All antibodies were used at 1:50 dilution.

In human cord blood, mononuclear cells were isolated using Ficoll-Paque PREMIUM (density 1.078, GE healthcare life science). Mononuclear cells were frozen down with 90% FBS and 10% DMSO in -80°C for further experiments. For flow cytometry study, frozen mononuclear cells were thawed and stained with human Hematopoietic Lineage FITC Cocktail (ebioscience), anti-human CD34-APC, CD38-PE cy7, CD90-Alexa 700 and CD45RA -Pacific Blue. Hematopoietic stem cells (HSCs) were defined as $\text{Lin}^- \text{CD34}^+ \text{CD38}^{\text{lo}} \text{CD90}^+ \text{CD45RA}^-$ cells⁷.

Phosphorylation flow cytometry of hematopoietic stem cell in human cord blood

CD34+ cells from human cord blood were isolated using magnetic beads (CD34 MicroBead Kit, human, Miltenyi Biotec) according to the protocol from manufacture. Cells were then treated with human recombinant TPO (20ng/ml) for 10 minutes at 37°C followed by wash with cold phosphate buffered saline (PBS) and permeabilized with a proprietary buffer (BD™ Phosflow Perm Buffer III; 558050, BD) on ice for 30 minutes. After two washes with PBS/FBS buffer (554657, BD), cells were incubated with antibodies to anti-human Stat5 (pY694)-PE (562007, BD), ERK1/2 (pT202/pY204)-PE (561991, BD) or AKT (Thr308) (9088S, Cell signaling), and analyzed by flow cytometry using a BD LSR-II flow cytometer⁸.

Cord blood genotyping, CD34+ cell enrichment from cord blood mononuclear cells and megakaryocyte colony forming unit (MK-CFU) assay

Genotyping of single nucleotide polymorphism (SNP) of Lnk rs3184504 of cord blood was performed using TaqMan® Assays (C_2981072_10, 4351379, Thermo Fisher). DNA was isolated from whole blood using DNA isolation column. Cord blood mononuclear cells isolated using Ficoll-Paque Premium was enriched with CD34+ cells using magnetic beads (CD34 MicroBead Kit, human, Miltenyi Biotec). MK-CFU was performed using a MegaCult™-C collagen-based assay (Stem cell Technologies). Briefly, a total of 5000 cells were seeded into a semi-collagen gel culture medium and cultured in two chamber slides for 12 days with cytokines including TPO (50ng/ml), IL-3 (10ng/ml) and IL-6 (10ng/ml). Cells were fixed with 1:3 methanol:acetone solution at room temperature for 20 minutes. Slides were stained using immunohistochemistry staining protocol by blocking the slides with human serum, incubating with anti-human GPIIb/IIIa primary antibody (1:100 dilution) and then a biotin-conjugated goat anti-mouse IgG secondary antibody (1:300 dilution), and finally colorized using avidin alkaline phosphatase conjugate. Last, the slides were counterstained with Evans Blue. CFU-Mk colonies usually ranged in size from three to several hundred megakaryocytes per colony. Small size colony referred to a colony with 3 to 20 cells per colony, while a medium or a large colony was defined as a colony with 21 to 49 cells per colony, or ≥ 50 cells per colony. Large Mk colonies arise from more primitive Mk progenitors whereas the smaller Mk colonies are produced from more mature Mk progenitors.

Immunoblot

Whole cell protein extracts were obtained by lysing platelets in Laemmli sample buffer (Bio-Rad) and heating to 100°C for 5 minutes. Samples were electrophoresed in 8% to 16% gradient Tris-glycine gels (Invitrogen) and transferred to nitrocellulose membranes, which were then blocked for 1 hour with blocking buffer (927-40000, Odyssey). Membranes were incubated with the appropriate primary antibody in Odyssey blocking buffer with 0.1% Tween 20 (16 hours, 4°C), washed with Tris-buffered saline-Tween 20 (TBST), and incubated with the anti-rabbit or anti-mouse HRP secondary antibody at room temperature for 30 minutes. Primary antibodies used included anti-phospho-p44/42 MAPK (p-Erk1/2) (Thr202/Tyr204), anti-p44/42 MAPK (Erk1/2), anti-phospho-AKT (Thy 308), anti-AKT (pan), anti-phospho-Stat5, anti-Stat5, anti PKC substrates (pSer), anti-phospho-SHIP1 (Tyr 1020), and anti-integrin β3 (all from Cell Signaling). Protein bands were detected using Supersignal West Pico-enhanced chemiluminescent solution (Pierce).

Platelet isolation and platelet aggregation function study using aggregometer

Platelet-rich plasma was prepared and platelets were pelleted with 1 μ M PGE1 to inhibit platelet activation. Platelet were resuspended in HEPES-buffered modified Tyrodes buffer (HBMT) at a concentration of 3.0×10^5 / μ l. After incubation in 37°C water bath for 30 minutes, platelet aggregation was initiated with AYPGKF (final concentration 100 μ M) or ADP (final concentration 20 μ M) and monitored in a PAP-8E aggregometer (BioData Corporation) at 37°C with stirring. The light transmission rate was recorded by the software.

Cholesterol loading on platelets using cholesterol-rich liposome

Cholesterol-rich liposome was prepared using a modified protocol⁹⁻¹¹. Briefly, 20mg, 40mg and 80mg cholesterol (Sigma) were mixed with 1,2-dimyristoyl-sn-glycero-3-phosphocholine(DMPC)(Avanti Polar Lipids) and dissolved in chloroform to make cholesterol-rich liposome. These cholesterol-rich liposomes were dried onto glass vessel walls under a stream of nitrogen gas and re-suspend in 10ml HBMT buffer which then were subjected to 70W for 45 minutes with a probe sonication at room temperature. The preparations were then centrifugated at 10,000 g for 20 minutes and supernatant was collected and store in aliquot at 4°C. The concentration of cholesterol-rich liposome was 2mg/ml, 4mg/ml and 8mg/ml respectively. Platelets were isolated from mice using the protocol mentioned above and re-suspended in 30 μ l HBMT and loaded with 30 μ l 2mg/ml, 4mg/ml and 8mg/ml cholesterol-rich liposome for 2 hours at 37°C before AYPGKF (Ala-Tyr-Pro-Gly-Lys-Phe-NH₂ peptide, PAR4 agonist, Sigma) stimulation at 100 μ M for 10 minutes.

Filipin staining of cell surface free cholesterol levels on platelets using both flow cytometry and confocal microscope

Platelets were isolated and washed with HBMT before stained with filipin for 2 hours. Samples then were run on LSR-II using DAPI channel. Imaging of filipin stained platelets was performed on an AxioObserver Z.1 microscope (Zeiss, Thornwood, NY) using a 100x/1.3 Plan-Neofluoar objective lens and an Orca ER cooled CCD camera (Hamamatsu Photonics, Bridgewater, NJ). Filipin was excited with a 365-nm LED (Zeiss Colibri) and emission was collected through a 455-nm beamsplitter and a 480/40 nm emission filter (Zeiss filter set 47 with excitation filter removed). Hardware was controlled by ZEN software (Zeiss).

Cholesterol content of platelets

Platelets were isolated and a small aliquot was saved to determine protein content using Pierce™ BCA Protein Assay Kit (23225, Thermo Scientific). Platelet total lipids were extracted using methanol/chloroform (v:v 1:2). The lipids in chloroform were then dried down under nitrogen gas and resuspended in 50 mM Tris, pH 7.5 and 0.1% Triton X-100. Total cholesterol content was measured using Cholesterol E kit (435-35801, Wako) and normalized to platelet protein content.

Reverse-transcriptase quantitative polymerase chain reaction (RT-qPCR) of *LNK*, *ATXN2*, *TRAFD1* and *PTPN11* mRNA levels in cord blood CD34⁺ cells

CD34⁺ cells from human cord blood were isolated using magnetic beads as mentioned above. Cells were harvested and RNAs were isolated using RNasey Mini kit (74104, Qiagen) according to the manufacturer's protocol. RNA with an A260/280 of >1.8 was used for cDNA synthesis using Maxima First Strand cDNA Synthesis Kit (K1671, Thermo Scientific) and qPCR was performed in a 7500 Real-Time PCR system (Applied Biosystem) using SYBR green chemistry. Primers were purchased from Integrated DNA Technologies. Forward primer for *LNK* was 5'-CCAGGAGAAGCACCTTGGT-3' and reverse primer for *LNK* was 5'-CGGACAGACATCTTTGAGG-3'. Forward primer for *ATXN2* was 5'-AGTTGTTGGCTCCAAATGTGA-3' and reverse primer for *ATXN2* was 5'-CATGTGCGGCATCAAGTACCA-3'. Forward primer for *TRAFD* was 5'-GACCAGGAAACTCGACTGTGT-3' and reverse primer for *TRAFD* was 5'-AGTCTCCATGTCAGATTTGGGAA-3'. Forward primer for *PTPN11* was 5'-CCGCTCATGACTATACGCTAAG-3' and reverse primer for *PTPN11* was 5'-AGACCGTTCTCTCCGTATTCC -3'. Forward primer for *CYC* was 5'-GCCATCCAACCACTCAGTCT-3' and reverse primer for *CYC* was 5'-ATGTGTCAGGGTGGTGACT-3'.

TPO mRNA levels in mouse liver, kidney and bone marrow

For RNA isolation from bone marrow cells, bone marrow cells were flushed out of tibia and wash twice with Hank's Balanced Salt Solution (HBSS) and lysed in RLT buffer from the kit of RNeasy Mini kit from Qiagen (74104, Qiagen). and RNAs were isolated according to the instruction from the manufacturer. For liver and kidney RNA isolation, 50mg tissues were homogenized in 1 ml of TRIZOL reagent using a power homogenizer. 0.2 ml of chloroform was added to the Trizol and undergone centrifugation at 15,000 xg for 10 minutes to separate phases. The top 200 ul from the top layer was collected and added to 700 ul of Qiagen

RLT buffer in a new tube. RNA isolation from RLT cell lysates from bone marrow, liver and kidney were isolated using RNeasy Mini kit. cDNA synthesis was performed using Maxima First Strand cDNA Synthesis Kit (K1671, Thermo Scientific) and qPCR was performed in a 7500 Real-Time PCR system (Applied Biosystem) using Taqman mouse TPO gene expression assay (Mm00456355_m1, 4331182, Thermo Fisher). GAPDH was used as internal control (Mm00186825_cn, 4400291, Thermo Fisher).

Allele-specific qPCR of C and T alleles of LNK expression levels

CD34⁺ HSCs from cord blood were isolated using using magnetic beads (CD34 MicroBead Kit, human, Miltenyi Biotec). RNA isolation and cDNA preparation were performed as mentioned above. The SNP genotyping TaqMan assays for allele-specific *LNK* probes and were provided by the Thermo Fisher (assay ID: C___2981072_10). Assay validation was performed by mixing a certain ratio of CC and TT homozygous samples and a standard curve was draw as reported in recently publication¹².

TPO uptake and enzyme-linked immunosorbent assay (ELISA) of TPO levels

Wash platelets were obtained as stated previously and resuspended in HBMT buffer. Platelets were then incubated with 2000 pg/ml recombinant TPO at °C for 1 hour. After incubation, platelets were palleted and the supernatant was used without further dilution in the Quantikine TPO ELISA. TPO uptake was calculated as follows: uptake%= (2000-ELISA read-out)*100/2000. TPO levels in plasma and HBMT buffer were measured using Mouse/Rat CCL2/JE/MCP-1 Quantikine ELISA Kit (DCP00, R&D) and Mouse IFN-gamma Quantikine ELISA Kit (MIF00, R&D) according to the manufacture's protocols.

Statistics

T-test was used in comparing the difference between two groups in the mouse studies. One-way ANOVA was used in comparing the difference among more than three groups in the mouse studies and cord blood sample analysis. The difference between two specific groups from one-way ANOVA was further analyzed using post-hoc Bonferroni test. For the analysis of genotype and diet/cholesterol loading interaction, two-way ANOVA was used. Two-tail analysis was performed in all statistical analysis except the gene expression levels in cord blood in supplementary figure 2 where one-tail t test was performed. p value less than 0.05 was considered as a significant difference.

References:

1. Bersenev A, Wu C, Balcerek J and Tong W. Lnk controls mouse hematopoietic stem cell self-renewal and quiescence through direct interactions with JAK2. *J Clin Invest*. 2008;118:2832-44.
 2. Wang Y, Wang GZ, Rabinovitch PS and Tabas I. Macrophage mitochondrial oxidative stress promotes atherosclerosis and nuclear factor-kappaB-mediated inflammation in macrophages. *Circ Res*. 2014;114:421-33.
 3. Li J, Vootukuri S, Shang Y, Negri A, Jiang JK, Nedelman M, Diacovo TG, Filizola M, Thomas CJ and Collier BS. RUC-4: a novel alpha1bbeta3 antagonist for prehospital therapy of myocardial infarction. *Arterioscler Thromb Vasc Biol*. 2014;34:2321-9.
 4. Wang W, Burg N, Vootukuri S and Collier BS. Increased Smad2/3 phosphorylation in circulating leukocytes and platelet-leukocyte aggregates in a mouse model of aortic valve stenosis: Evidence of systemic activation of platelet-derived TGF-beta1 and correlation with cardiac dysfunction. *Blood Cells Mol Dis*. 2016;58:1-5.
 5. Wang W, Oh S, Koester M, Abramowicz S, Wang N, Tall AR and Welch CL. Enhanced Megakaryopoiesis and Platelet Activity in Hypercholesterolemic, B6-Ldlr^{-/-}, Cdkn2a-Deficient Mice. *Circ Cardiovasc Genet*. 2016.
 6. Murphy AJ, Bijl N, Yvan-Charvet L, Welch CB, Bhagwat N, Reheman A, Wang Y, Shaw JA, Levine RL, Ni H, Tall AR and Wang N. Cholesterol efflux in megakaryocyte progenitors suppresses platelet production and thrombocytosis. *Nat Med*. 2013;19:586-94.
 7. Pang WW, Price EA, Sahoo D, Beerman I, Maloney WJ, Rossi DJ, Schrier SL and Weissman IL. Human bone marrow hematopoietic stem cells are increased in frequency and myeloid-biased with age. *Proc Natl Acad Sci U S A*. 2011;108:20012-7.
 8. Wang W, Vootukuri S, Meyer A, Ahamed J and Collier BS. Association between shear stress and platelet-derived transforming growth factor-beta1 release and activation in animal models of aortic valve stenosis. *Arterioscler Thromb Vasc Biol*. 2014;34:1924-32.
 9. Shiraishi M, Tamura K, Egoshi M and Miyamoto A. Cholesterol enrichment of rabbit platelets enhances the Ca(2+) entry pathway induced by platelet-derived secondary feedback agonists. *Life Sci*. 2013;92:838-44.
 10. Shiraishi M, Tani E and Miyamoto A. Modulation of rabbit platelet aggregation and calcium mobilization by platelet cholesterol content. *J Vet Med Sci*. 2010;72:285-92.
 11. Sorisky A, Kucera GL and Rittenhouse SE. Stimulated cholesterol-enriched platelets display increased cytosolic Ca²⁺ and phospholipase A activity independent of changes in inositol trisphosphates and agonist/receptor binding. *Biochem J*. 1990;265:747-54.
 12. Soldner F, Stelzer Y, Shivalila CS, Abraham BJ, Latourelle JC, Barrasa MI, Goldmann J, Myers RH, Young RA and Jaenisch R. Parkinson-associated risk variant in distal enhancer of alpha-synuclein modulates target gene expression. *Nature*. 2016;533:95-9.
-

Supplemental Figure Legend

Supplementary Fig. I: p-AKT levels in CD34⁺ cells from cord blood.

Supplementary Fig. II: *LNK*, *ATXN2*, *TRAFD1* and *PTPN11* mRNA levels in cord blood CD34⁺ cells. (a) *LNK*, (b) *ATXN2*, (c) *TRAFD1* and (d) *PTPN11*. (p values of one-tail t-test were reported).

Supplementary Fig. III: Allele specific PCR to quantify the mRNA levels of *Lnk* with either C or T alleles. Allele-specific *LNK* expression analysis of allele-biased samples with indicated allele ratios to verify the assay.

Supplementary Fig. IV: *Lnk*^{-/-} BM recipient mice had leukocytosis and lymphocytosis. The BM recipient mice were fed with chow (black bars) or WTD (green bars) for 12 weeks. *** p<0.01 and <0.001 between donor genotype (WT→WT vs. *Lnk*^{-/-}→WT, or WT→*Ldlr*^{-/-} vs. *Lnk*^{-/-}→*Ldlr*^{-/-}). ^^<0.001 between recipient genotype (diet) (WT→WT vs. WT→*Ldlr*^{-/-}, or *Lnk*^{-/-}→WT vs. *Lnk*^{-/-}→*Ldlr*^{-/-}).

Supplementary Fig. V: Time course of plasma cholesterol levels in mice fed with WTD.

Supplementary Fig. VI: Washed platelet aggregation.

The BM recipient mice were fed with chow (black line) or WTD (green line) for 12 weeks. Shown are representative of washed platelet aggregation. (a) PAR4 agonist (AYPGKF 100μM) induced aggregation and (b) ADP induced aggregation.

Supplementary Fig. VII: TPO mRNA levels in liver, kidney and bone marrow from mice on WTD or chow diet.

Supplementary Fig. VIII: Cholesterol content of platelets from mice on WTD or chow diet. (a) flow cytometry of Fillipin stained platelets for free cholesterol estimation. (b) total cholesterol levels in platelets. (c) confocal microscope of Fillipin stained platelets. Abbreviations: n.s. not significant.

Supplementary Fig. IX: PKC activity of platelets in response to PAR4 agonist (AYPGKF) stimulation. Platelets from chow-fed (WT→WT and *Lnk*^{-/-}→WT) or WTD-fed (WT-*Ldlr*^{-/-} and *Lnk*^{-/-}→*Ldlr*^{-/-}) recipients were stimulated with AYPGKF (100 μM) for 10 min and PKC activity was estimated by Western analysis.

Supplementary Fig. X: western blot quantification of signaling in platelets. (a) p-Akt in resting and AYPGKF activated platelets and **(b)** p-SHIP-1 in AYPGKF activated platelets of chow-fed (WT→WT and *Lnk*^{-/-}→WT) or WTD-fed (WT-Ldlr^{-/-} and *Lnk*^{-/-}→Ldlr^{-/-}) recipients.

Supplementary Fig. XI: effect of ex vivo cholesterol loading on p-SHIP1 from platelets of chow fed mice.

Supplementary Fig. XII: Quantification of tolimidone effect on p-Akt in WT and *Lnk*^{-/-} platelets from chow diet fed mice.

Supplementary Fig. XIII: Quantification of p-SHIP1 in platelets from both WT and *Lyn*^{kd/kd} mice after AYPGKF stimulation.

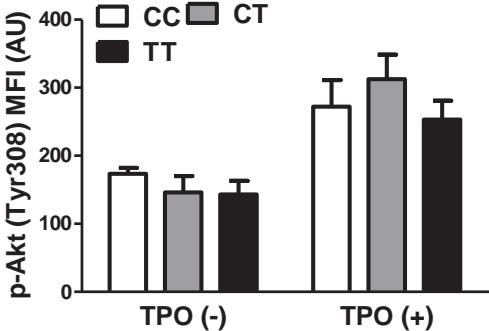
Supplementary Fig. XIV: Diastolic (a) and systolic (b) blood pressure in WT and *Lnk*^{-/-} BM recipient mice on WTD diet for 10 weeks.

Supplementary Fig. XV: Glucose (a) and insulin (b) levels of WT and *Lnk*^{-/-} BM recipient mice.

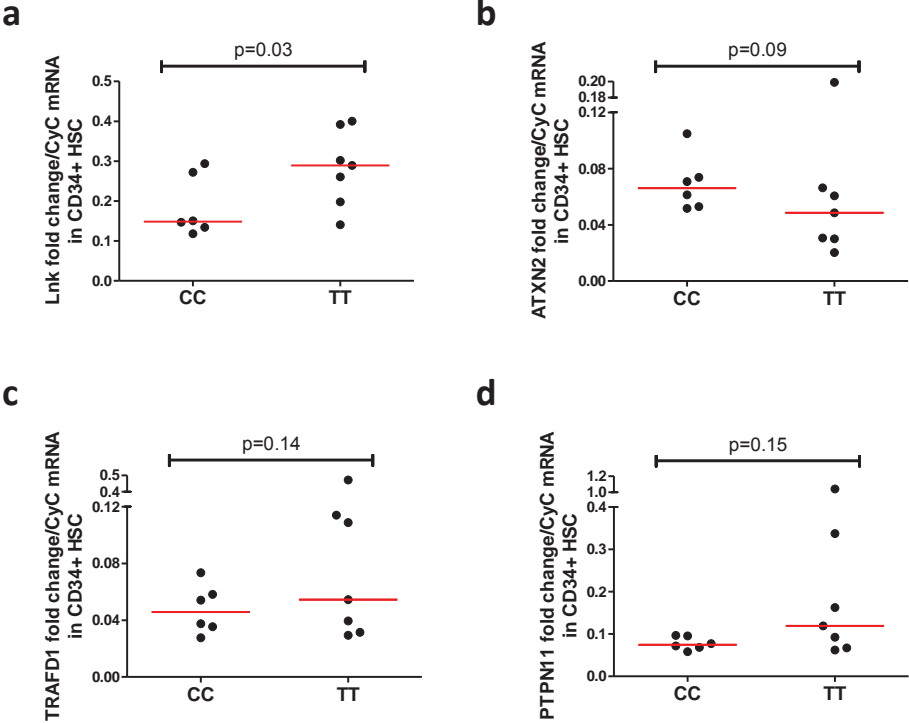
Supplementary Fig. XVI : Plasma MCP-1 levels of WT and *Lnk*^{-/-} BM recipient mice on WTD for 10 weeks.

Supplementary Fig. XVII: CD3⁺ T-cells of atherosclerotic lesion of WT and *Lnk*^{-/-} BM recipient mice. (a) quantification and (b) representative images.

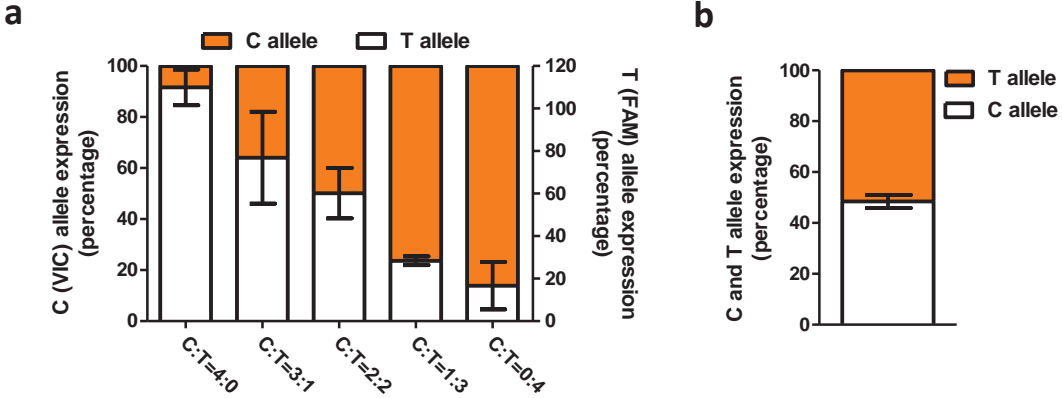
Supplementary Fig.1



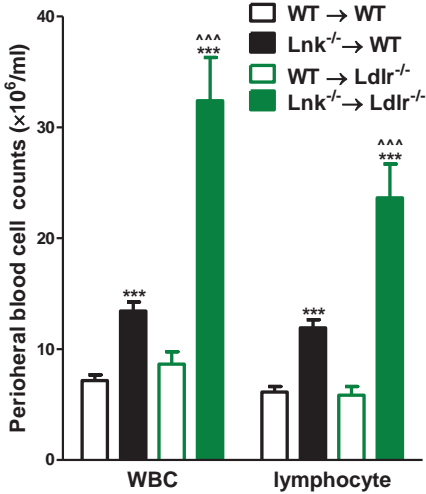
Supplementary Fig. II



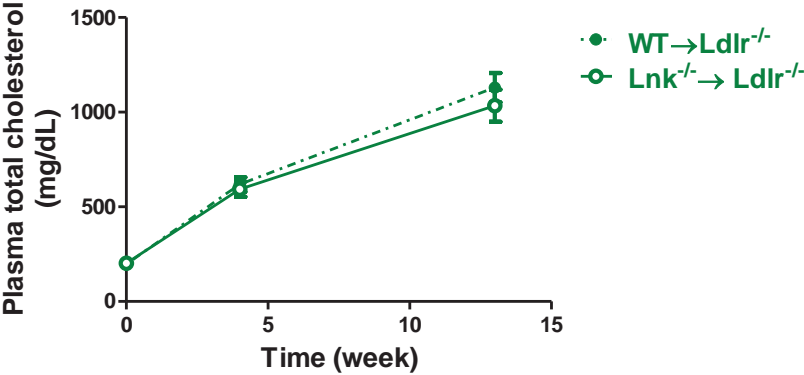
Supplementary Fig. III



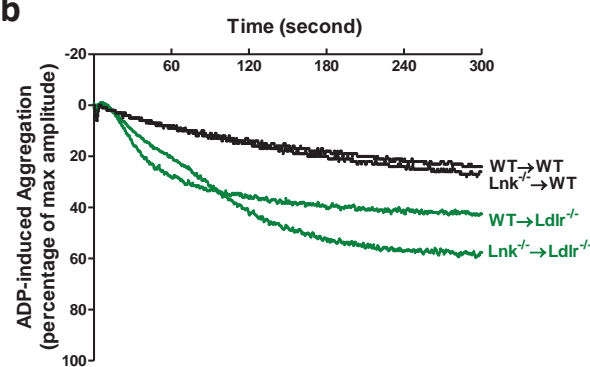
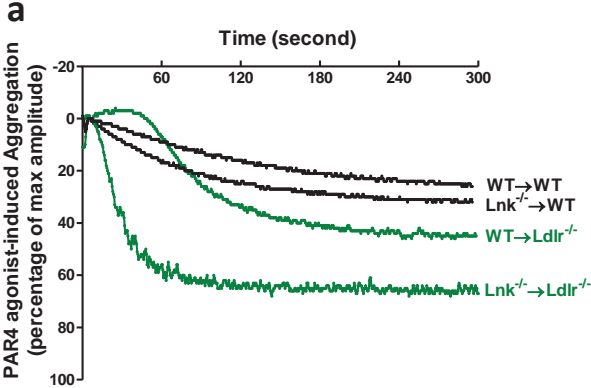
Supplementary Fig. IV



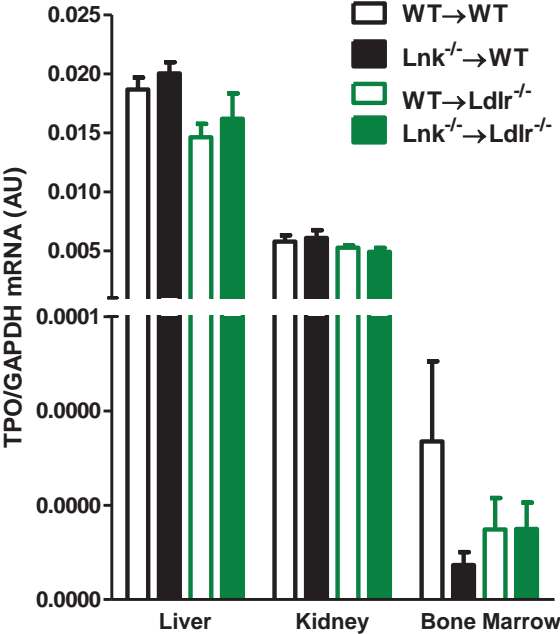
Supplementary Fig. V



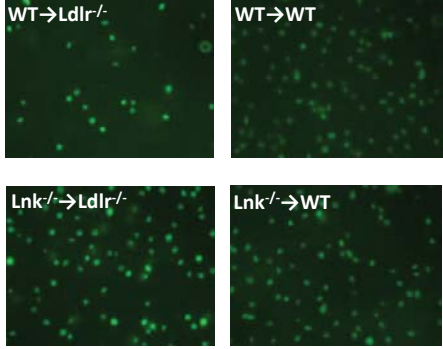
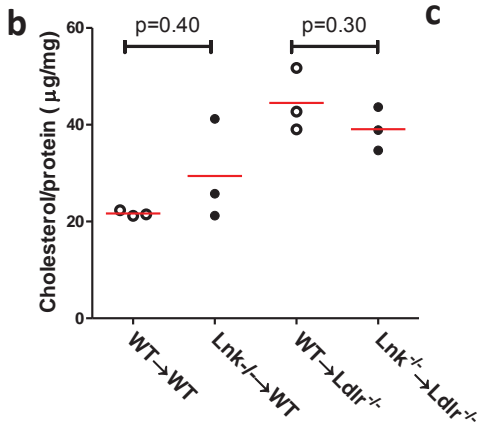
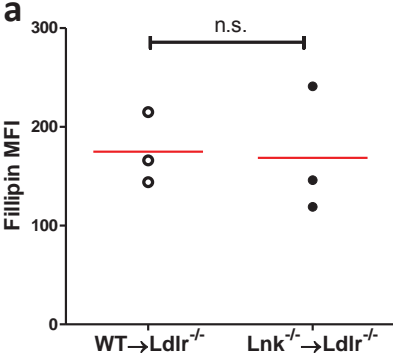
Supplementary Fig. VI



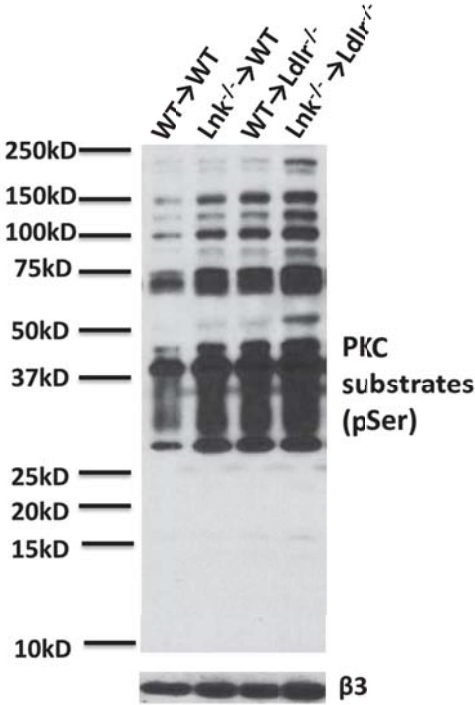
Supplementary Fig. VII



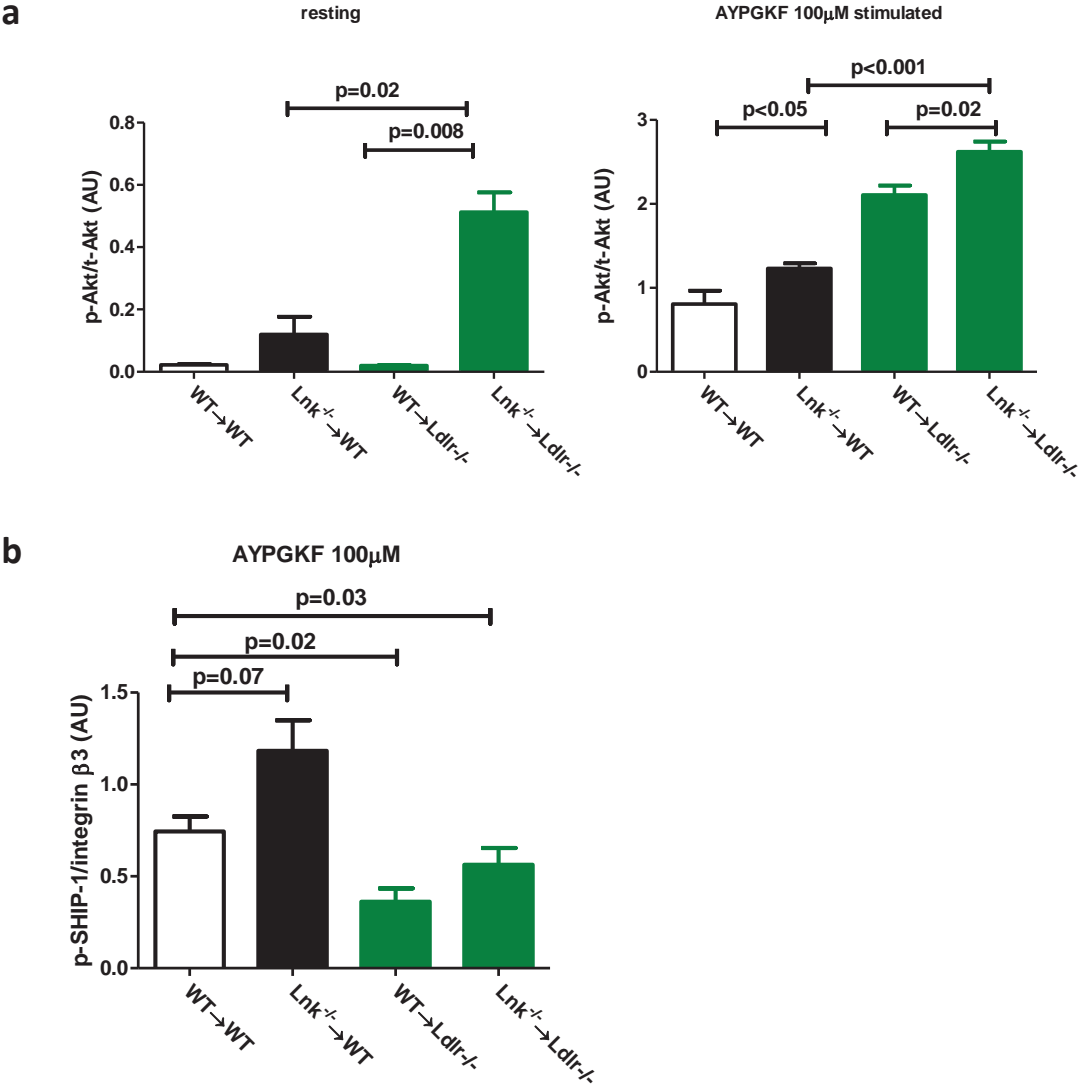
Supplementary Fig. VIII



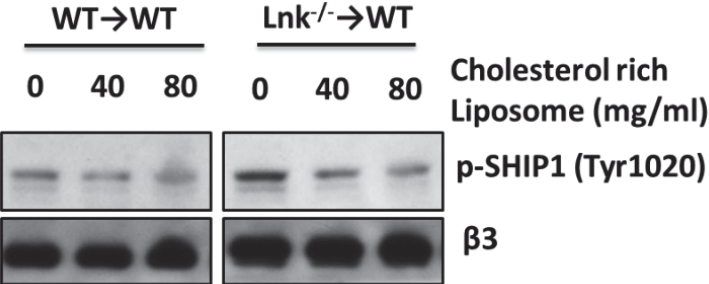
Supplementary Fig. IX



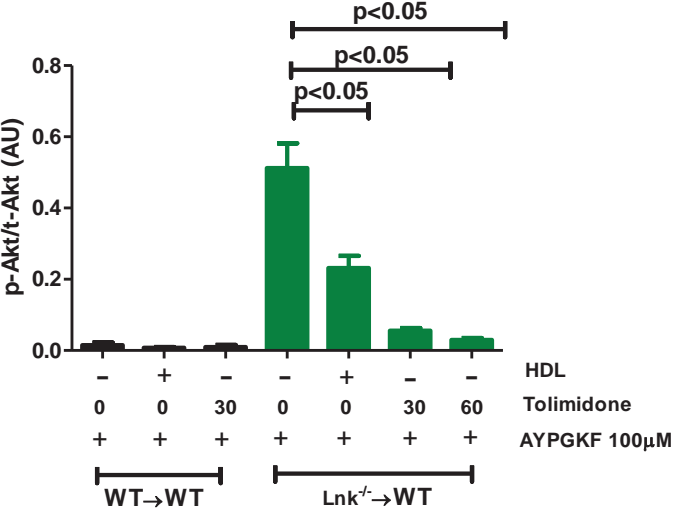
Supplementary Fig. X



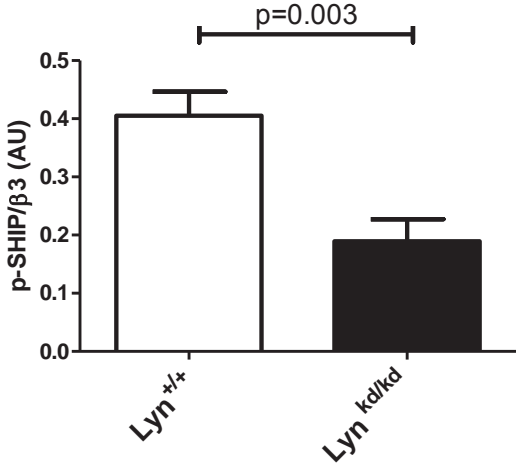
Supplementary Fig. XI



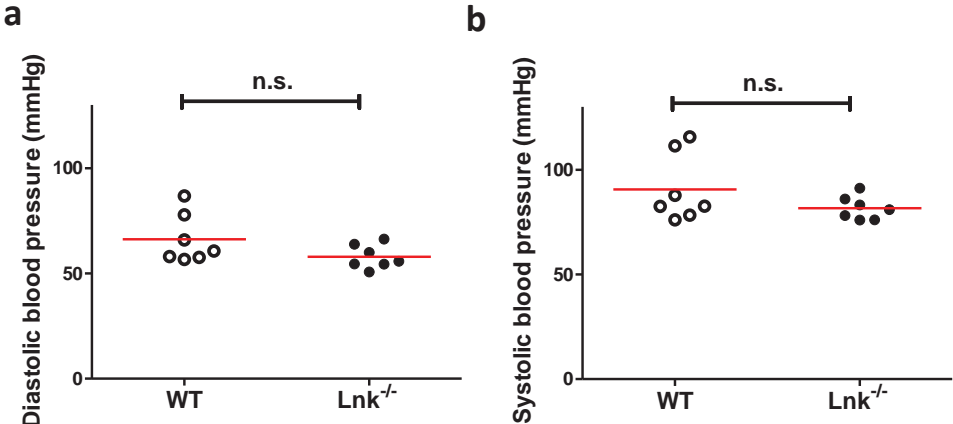
Supplementary Fig. XII



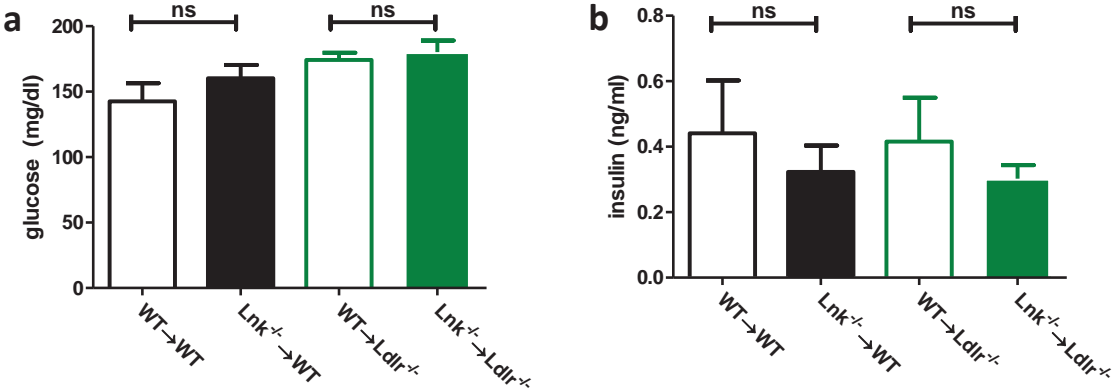
Supplementary Fig. XIII



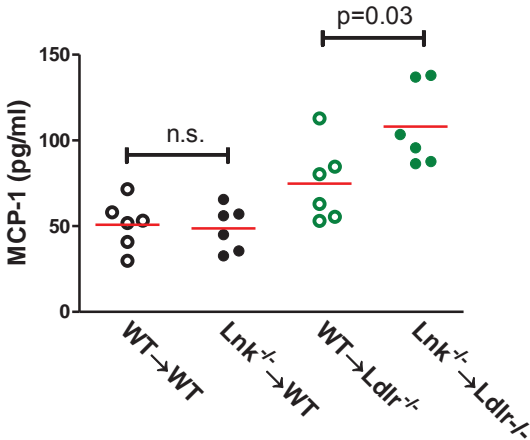
Supplementary Fig. XIV



Supplementary Fig. XV



Supplementary Fig. XVI



Supplementary Fig. XVII

